Forgotten linear behaviours in the sound field

[1] Yoshimasa Sakurai and [2] Hiroshi Morimoto

[1] Experimental House, 112 Gibbons Rd, Kaiwaka 0573
Email: yoshi@ecohouse.co.nz
[2] Suisaku Ltd, 21-1 Mihara-cho Kodera, Minami kawachi-gun, Osaka, Japan

Abstract

First reflections of a rigid panel, a rigid concave and convex panel, and a panel with reflection coefficient are reviewed as well as multiple reflections between them. Thus, early reflections in a scale model auditorium were calculated and compared with measured results. The transient response of human hearing system in the form of impulse response with 0.05ms rectangular pulse wave is reviewed. It has the absolutizing process after the linear response. Familiar impact sounds got pair comparison to arrange on the axis of loudness. When each impact sound was convolved with the dB (A) weight and the transient response of our hear-ing system, it was found that the latter convolution showed larger correlation to each loudness. And it was found that the time window of 40ms gives the largest correlation for its loudness among other time windows. The measurement of angle discrimina-tion was done with a 0.05ms rectangular pulse. It exists where the cross correlation of HRTF is 0.98. Acoustical information can be smoothed in this space. If it is expressed in the space using the stereoscopic view, temporal information is also obtained. It can be compared with the given estimation of a concert hall. Acoustical behaviours must be first arranged and established as the linear system on a 0.05ms rectangular pulse, then further steps can be clearer.

Originally published in the 22nd Biennial Conference of the Acoustical Society of New Zealand, November 2014

1. Introduction

The impulse response of a linear system is the output of the delta function input and it is the fundamental response of the system to be convolved to a practical input to find its output. This behaviour exists in our hearing system as well as in a sound field. The process of absolutization occurs after it. In this paper, the line-ar behaviours of a sound field and hearing system are reviewed first and the time window for the loudness of an impact sound and the angular discrimination for a 0.5ms rectangular pulse is mentioned.

2. The early reflections of th impulse respose in an auditorium

On the boundary in a sound field, the integral equations are formulated [1] to obtain the rigorous solution. At present it has to be solved numerically and it is difficult to find intuitively from the result how a sound field is formed and characterized. The successive substitution in one of the equations, however, gives the multiple integrations with known functions which correspond to multiple reflections between boundaries.

A velocity potential $\Phi(P)$ at a point P in an enclosure F is expressed by Helmholtz-Kirchhoff integral [2],

$$\Phi(P) = \Phi_D(P) + \int\int_F \left\{\phi(q)\frac{\partial G}{\partial n} - \frac{\partial \phi(q)}{\partial n}G\right\} dS \qquad (1)$$

where $\Phi_D(P)$ is a direct wave from an omnidirectional point source at P_s, G is $exp(-ikr)/4\pi r$, where r is a distance from a point q on the boundary to a receiving point P, n is an inward normal, and $\emptyset(q)$ and $\delta\emptyset(q)/\delta n$ take values at the boundary. But they are not given. When a receiving point P converges to a point p on the boundary, Eq. (1) turns into the integral equation jumping $1/2\,\emptyset(p)$ because of the discontinuity of the double layer term [1],

$$\Phi(p) = 2\Phi_D(p) + 2\int\int_F \left\{\phi(q)\frac{\partial G}{\partial n} - \frac{\partial \phi(q)}{\partial n}G\right\} dS \qquad (2)$$

where k is a wave number and an admittance A_j on a surface j is defined as,

$$\frac{\partial \phi}{\partial n} = ikA_j\phi \qquad (3)$$

and the surface F is composed of N different parts, the successive substitution in Eq. (2) yields,

$$\begin{aligned}\Phi(p) = 2\Phi_D(p) &+ \sum_{j=1}^{N}\Big[2\int\int_{F_j}\Big\{2\phi_D(q)\frac{\partial G}{\partial n} - ikA_j 2\phi_D(q)G\Big\}dS_j\Big] \\ &+ \sum_{k=1}^{N} 2\int\int_{F_k}\Big[\sum_{j=1}^{N} 2\int\int_{F_j}\Big\{\phi(q)\frac{\partial G}{\partial n} - ikA_j 2\phi_D(q)G\Big\}dS_j\frac{\partial G}{\partial n} \\ &- ikA_k\Big\{\sum_{j=1}^{N} 2\int\int_{F_j}\Big(\phi(q)\frac{\partial G}{\partial n} - ikA_j\phi(q)G\Big)dS_j\Big\}\Big]dS_k + \cdots \end{aligned} \qquad (4)$$

A velocity potential at a receiving point P is obtained by the substitution of Eq. (4) into Eq. (1),

$$\Phi(P) = \Phi_D(P) + \sum_{j=1}^{N} \int\int_{F_j} 2\phi_D \left\{ \frac{\partial G}{\partial n} - ikA_j G \right\} dS_j + \sum_{k=1}^{N} \int\int_{F_k} \sum_{j=1}^{N} \left[2 \int\int_{F_j} \cdot 2\phi_D \left\{ \frac{\partial G}{\partial n} - ikA_j G \right\} dS_j \right] \cdot \left\{ \frac{\partial G}{\partial n} - ikA_k G \right\} dS_k + \cdots \quad (5)$$

or

$$\Phi(P) = \Phi_D(P) + \sum_{j=1}^{N} \int\int_{F_j} 2\phi_D \frac{\partial G}{\partial n} R_j dS_j + \sum_{k=1}^{N} \int\int_{F_k} \sum_{j=1}^{N} \left[2 \int\int_{F_j} 2\phi_D \frac{\partial G}{\partial n} R_j dS_j \right] \cdot \frac{\partial G}{\partial n} R_k dS_k + \cdots \quad (6)$$

where

$$R_j = 1 + \frac{ikA_j}{(ik + 1/r)\cos(n.r)} \quad (7)$$

R_j is called a reflection coefficient. Each term in the right hand side shows a direct sound, the first and second reflections, respectively. When a surface is rigid and A_j is zero, R_j becomes unity. The second term in the right hand side of Eq. (6) in that case can be separated into two terms. Each of them can be transformed into the line integral [3] as is shown in Eq. (8). The multiple surface integrals between plane panels in Eq. (6) are then reduced to the line integrals. Practical calculations of multiple integrals, multiple reflections between different kinds of panels are mentioned as well.

2.1 First reflections of boundaries in an auditorium

1) The reflection of a rigid plane panel [4]

The first reflection of a rigid plane panel in Figure 1 corresponds to the second term in Eq. (6) when R_J is equal to unity. In the time domain, the reflection of the rigid plane panel, $h(P,t)$ is expressed

$$h(P,t) = \frac{\delta(t - d/C)}{d} + \frac{\delta(t - d'/C)}{d'} + \frac{1}{4\pi} \int_{\Gamma} \frac{\delta(t - (r + r_s)/C)}{r r_s} \cdot \left\{ \frac{\boldsymbol{r} \times \boldsymbol{r}'_s}{r r'_s + \boldsymbol{r} \cdot \boldsymbol{r}'_s} + \frac{\boldsymbol{r} \times \boldsymbol{r}_s}{r r_s + \boldsymbol{r} \cdot \boldsymbol{r}_s} \right\} \cdot d\boldsymbol{g} \quad (8)$$

,where $\delta(t)$ is a delta function and C is a sound velocity.r_s, r_s' and r are vectors from a point source, an image source and a receiving point to the edge, respectively. dg is an element of a vector tangential to the edge. ε takes one, one half and zero, when a receiving point P is inside, on and outside the cone formed by P_s' and F in Figure 1, respectively. In the right hand side of Eq. (8), the first term is a direct sound from a point source, the second term is a geometrical wave from the image source P_s' and the third term is the edge waves from the image and real sources. The first term of the line integral corresponds to the diffracted wave from a complementary opening with the Kirchhoff's boundary condition which produced the direct sound from the image source. The equation shows that there is no reflection other than the geometrical wave until the wave front reaches the edges of the panel. Edge waves have a role to express the dimension of a panel and the ge-ometrical relation.

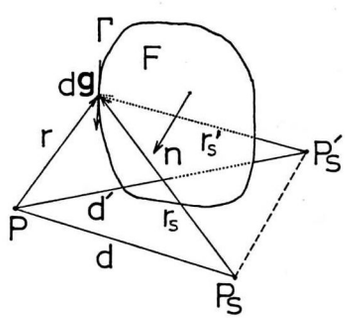

Figure 1: Sound reflection of a rigid plan panel by the in integral along Γ. A point source is at P_s and a receiving point is at P. P_s' is the image sources of P_s; n is the inward normal of the panel; d, d' are distances from the point source and the image source to the receiving point, respectively.

When the panel has a specular reflection point on it, they are negative. These negative waves becomes larger and closer to the specular reflection, as a panel become smaller. This explains our daily experience to hear only a small reflection from a small rigid panel even if it has a specular reflection. The next two points are very important for the later calculation of the multiple reflections between panels. The geometrical wave is the contribution of the singular point which is at a specular reflection point on a reflecting panel. A line element dg of the line integral, it is a secondary point source with directivity.

2) The reflection of a rigid curved panel [5]

If the rigid plane panel in Figure 1 is surrounded by other rigid panels, the last term of the line integrals in Eq. (8) vanishes on the common sides because of the counter line integral. Even at the free edges, it is less effective than the first term on the reflection side.

If a curved rigid panel in Figure 2 is parcelled into the partitions where an incident spherical wave can be regarded as a plane one and the curvature is estimated to be flat in comparison with a wavelength, and an asymptotic expansion, i.e. Fraunhofer diffraction, is applied to the surface integral corresponding to the remaining first term.

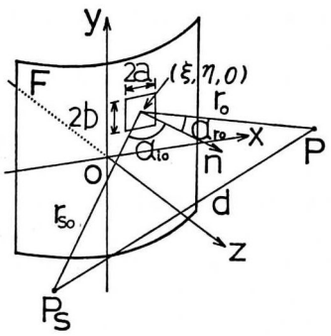

Figure 2: Sound reflection of a curved rigid panel. A point source P_s is at (x_0, y_0, z_0) and the receiving point P is at (x,y,z); side lengths of a division are $2a$ and $2b$; α_{i0} and α_{r0} are incident and reflection angles at the centre of division which is at (ξ,η,0), respectively; r_{s0} and r_0 are distances from the point source and the receiving point to the centre, respectively.

The first reflection $h(P,t)$ of the curved rigid panel is approximately calculated by superposing the first reflections of the partitions as in the following,

$$h(P,t) = \frac{1}{4\pi}\sum_{j=1}^{N}[A_1\{U(t-T_1)+U(t-T_2) - U(t-T_3)+U(t-T_4)\}+A_2\{R(t-T_1) - R(t-T_2)+R(t-T_3)+R(t-T_4)\}], \quad (9)$$

where

$$A_1 = Cr_{s0}r_0(\cos\alpha_{i0}+\cos\alpha_{r0}) / [\{r_0(\eta-y_0)+r_{s0}(\eta-y)\}\cdot\{r_0(\xi-x_0)+r_{s0}(\xi-x)\}], \quad (10)$$

$$A_2 = C^2(r_0\cos\alpha_{i0}+r_{s0}\cos\alpha_{r0}) / [\{r_0(\eta-y_0)+r_{s0}(\eta-y)\}\cdot\{r_0(\xi-x_0)+r_{s0}(\xi-x)\}], \quad (11)$$

and

$$T_1 = -D_1-D_2+D_3,\ \ T_2 = -D_1+D_2+D_3,$$
$$T_3 = D_1-D_2+D_3$$

and

$$T_4 = D_1+D_2+D_3, \quad (12)$$

where

$$D_1 = \frac{a}{C}\{(\xi-x_0)/r_{s0}+(\xi-x)/r_0\},$$
$$D_2 = \frac{b}{C}\{(\eta-y_0)/r_{s0}+(\eta-y)/r_0\}$$

and

$$D_3 = (r_{s0}+r_0)/C+d/C \quad (13)$$

The far field term yields the step function $U(t)$ and the near field term yields the ramp functions $R(t)$. Figure 3 shows the reflection from a partition of the near and far field terms. When it is divided small, T_1,T_2,T_3 and $T4$ in Figure 3 come close each other and the height of the trapezoid wave becomes small. On the other hand, the far field term remains predominant having two rectangular waves with the opposite signs in the same height.

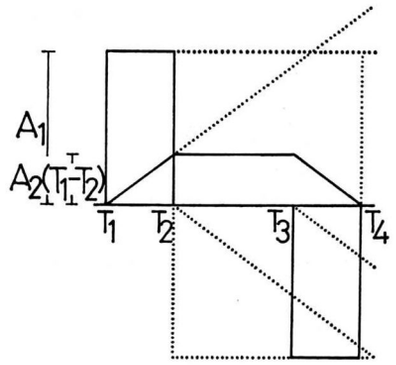

Figure 3: Reflection in the time domain from a rigid panel rectangular partition at a plane wave incidence. Far field terms: step functions, producer a pair of rectangular waves; near field terms: ramp functions, produce a trapezoid wave.

When the partition at the specular reflection on a rigid panel is surrounded by other partitions, the latter negative wave is cancelled completely in the case of a rigid plane panel, or almost completely in the case of a rigid convex panel, by the following positive waves from the other partitions (see Figure 4(a)). The partitions at the edges leaves boundary waves. When a panel is rigid and concave, positive and negative waves tend to be increased by those following in phase (see Figrue 4 (b)).

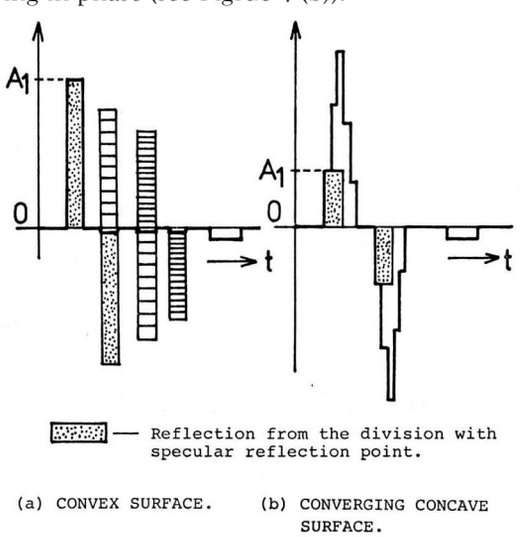

Figure 4: Formation of the specular reflections from a rigid concave or convex surface. A wave with a thick line shows the resultant.

3) The reflection of a plane panel covered with material having reflection coefficient [6].

The first reflection $h(P,t)$ of a plane panel covered with reflection coefficient in Figure 5 is practically obtained, substituting the reflection coefficient at the specular reflection $\gamma_0(t)$ for the other part of the surface,

$$h(P,t) = \gamma_0(t) * g(P,t), \quad (14)$$

where, $\gamma_0(t)$ is the reflection coefficient in the time domain at the specular reflection point on the panel with large dimension, $g(P,t)$ is the reflection of a rigid plane panel at the same position as the panel. * shows the convolution product.

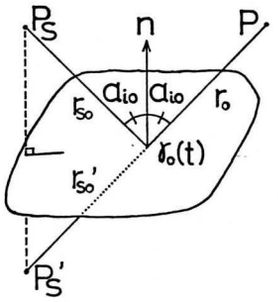

Figure 5: Sound reflection of a plane panel covered with reflection coefficient. $\gamma_0(t)$ is the reflection coefficient at the specular reflection where an incidence angle is α_{i0}.

Reflection coefficient at a specular reflection is obtained experimentally from the reflection of a sufficiently large plane panel covered with the material by de-convolving it from the direct sound of the image source. It shows the reflection of the surface when it is impinged by the impulsive spherical incident wave. Reflection coefficient in the time domain for punch-carpet and urethane form surface at different incident angles which are measured using spark pulses are shown in Figure 6. Unit in the ordinate corresponds to the reflection coefficient of a rigid surface, namely, the direct sound from the image source. Punch-carpet reflects more surface reflection because of harder surface, i.e., more impedance mismatching.

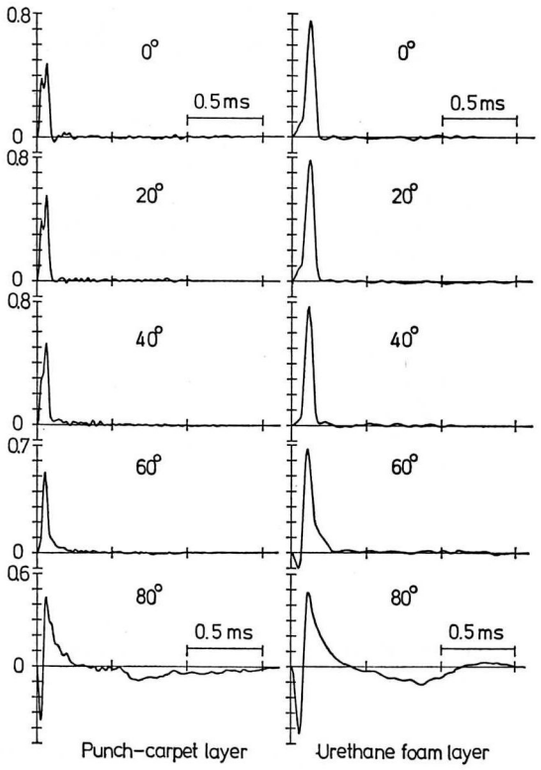

Figure 6: Reflection coefficients in the time domain of a punch-carpet layer of 4mm thickness and a urethane foam layer of 10mm thickness. An incidence angle is shown in each figure.

Reflection coefficient of a porous layer explains separately the amount of surface reflection and the reflection from its back with the amount decreased in the layer. It is interesting that at the grazing angle, both reflect negative surface reflections. This negative surface reflection can be imagined from the reflection coefficient for the plane wave incidence with the local reaction assumption.

When an incident angle is close to $\pi/2$, it becomes negative and its inverse Fourier transform yields negative reflection. Measured reflection coefficients for hard and soft real auditorium seats are reported [7]. They also have negative surface reflections at the grazing angles with the successive reflections among the seats. This negative reflection decreases the loudness of the direct sound from the stage. We have to notice the steep slope 26.3 degrees of auditorium seats at Greek amphitheatre [8] as shown in Figure 7.

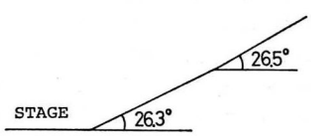

Figure 7: Steep slope of audience seats at a Greek ampitheatre

2.2 Multiple reflections between panels

1) Those between rigid plane panels [9]

The multiple reflection between rigid plane panels can be obtained from the interpretation of the first reflection mentioned in the earlier section.

When the projection of panel F_1 onto a panel F_2 from an image source P_s' covers F_2 as in Figure 8(a), the second reflection of a geometrical wave is obtained by the first reflection from F_2 of the image source P_s'. When it cuts F_2 by F_2' as in Figure 8(b), the second reflection is the first reflection from the area F_2'.

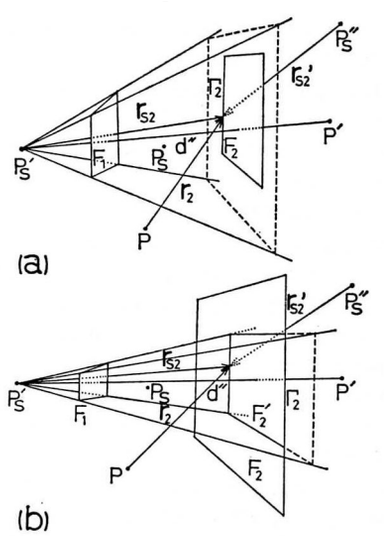

Figure 8: Second reflection of a geometrical wave having its boundary waves: (a) at the second panel F_2 and (b) on the projection F_2' of the first panel F_1 to the second panel F_2.

A higher order reflection of a geometrical wave can be estimated by the first reflection of the last image source from a panel or the area on the panel projected through the effective part of the preceding panel.

Since a geometrical wave is calculated as the contribution from the singular point on a second panel, the geometrical reflection of the edge wave at each element d_g is also obtained by finding the singular point on a second panel F_2 corresponding to it. Edge waves reflected at the edges of F_1 have such singular points on the lines $A'B'$, $B'C'$ and $C'D'$ on F_2 as shown in Figure 9. Geometrical reflection as the second reflection of edge waves is estimated by the line integrals Eq. (1) along AB, BC and CD of the panel F_1, when a point source is at P_s and a receiving point is at P' which is the image of a receiving point P. When the second edge reflection of edge waves at the first reflection is not negligible, it can be obtained by the double line integral.

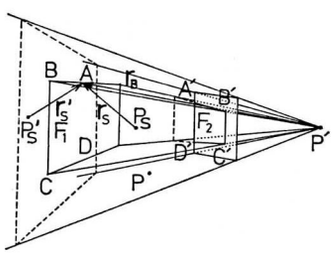

Figure 9: Geometrical reflecting of boundary waves. $A'B'$, $B'C'$ and $C'D'$ on F_2 have the specular reflections of the boundary waves at the first panel to the receiving point P'. r_s , r_s' and r_B are distances from the point source and its image sources, and the image receiving point on the edge, respectively.

2) Those between rigid curved panels [10]

2.1) Convex panels

Sound reflection from a rigid convex panel or concaved panel with small curvature is very similar to that from a rigid plane panel, when considered from the point of view that it produces a discrete specular reflection and a very slight reflection until a wave front reaches an edge. This suggests that the same treatment for calculating multiple reflection between rigid plane panels can be applied using an equivalent image point source as in Figure 10. The reflection at the specular reflection point on the second rigid curved panel from the first one is estimated by Eq.(9).

It has the magnitude of that from an equivalent image point source for the tangential plane at the specular reflection point of the first panel, as shown in Figures. 10(b) and (c). The second reflection between two rigid curved panels is approximated by the first reflection from one of them with the equivalent image point source thus obtained. This procedure corresponds to the calculation of the multiple reflection of a geometrical wave between rigid plane panels.

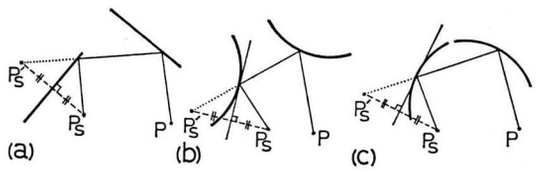

Figure 10: Multiple reflections between curved surfaces with equivalent image point sources for (b) a convex surface and (c) a concave surface.

2.2) Inside a concave panel with large curvature

At the second reflection inside the concave panel, the contribution from the division about the specular reflection point is still the most prominent, and the errors caused by the different incident angles of other partitions are decreased [10] by replacing them the incident angle of the specular reflection. For a second reflection, an image point source P_s' is obtained as for the tangential plane at the first specular reflection point as in Figure 11.

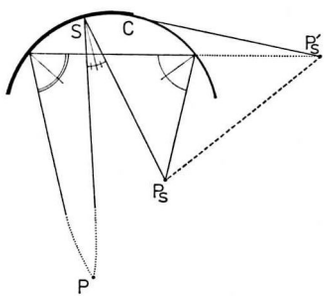

Figure 11: Multiple reflections inside a concave panel.

The plane of contact including the image P_s' limits an edge of the second reflecting concave panel, and the first reflection of the panel from the image source P_s' is convolved with the reflection from the point source to the second specular reflection point. The later continuous inter-reflection inside the curvature cannot be calculated with this method, but the calculation gives an approximate result to give good information. Its rigorous solution can be obtained by the integral equation methods.

3) Those between panels covered with materials having reflection coefficient other than unity [11]

The second reflections between two plane panels with reflection coefficients other than unity are also estimated by separating the first reflection of one of the panels. One is the contribution around the specular reflection point and another is lined point sources of edge waves at the edges (see Eqs. (8) and (14)). When two panels in Figure 12 are covered with reflection coefficients, both of them have specular reflection points, and the reflection of them as rigid surface is $g(P,t)$, their reflection is approximately estimated as,

$$h(P,t) = \gamma_{10}(t) * \gamma_{20}(t) * g(P,t), \qquad (15)$$

where $\gamma_{10}(t)$ and $\gamma_{20}(t)$ are reflection coefficients of two panels. Even if they do not have any specular reflection points on them, the reflection coefficients at the specular reflection points on their expanded surfaces are practically substituted.

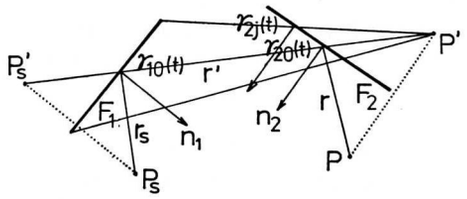

Figure 12: Multiple reflections between panels covered with reflections coefficients.

For the second reflection of the edge waves produced on the panel F_1 only their specular reflection on the panel F_2 is estimated. When the reflection coefficient at the incident angle of the edge waves on the panel F_1 which reflect specularly on the panel F_2 is $\gamma_{2j}(t)$ as shown in Figure 12, the reflection coefficient on the panel F_1 is $\gamma_{10}(t)$, and the specular reflection of the edge waves as the rigid surfaces is $g_{2j}(P,t)$, the specular reflection from the panel F_2 of the edge waves at the panel F_1, $h_2(P,t)$ is

$$h_2(P,t) = \sum_{j=1}^{m_2} \gamma_{10}(t) * \gamma_{2j}(t) * g_{2j}(P,t), \qquad (16)$$

where m_2 is the number of sides of the specular reflection on the panel F_2.

2.3 Early reflections in a scale model auditorium [12]

We are now ready to estimate the early reflections of the impulse response in an auditorium.

1) Experiments in the scale model auditorium

The scale model of an auditorium is made by the folded plane panels except the convex ceiling under the balcony as shown in Figure 13.

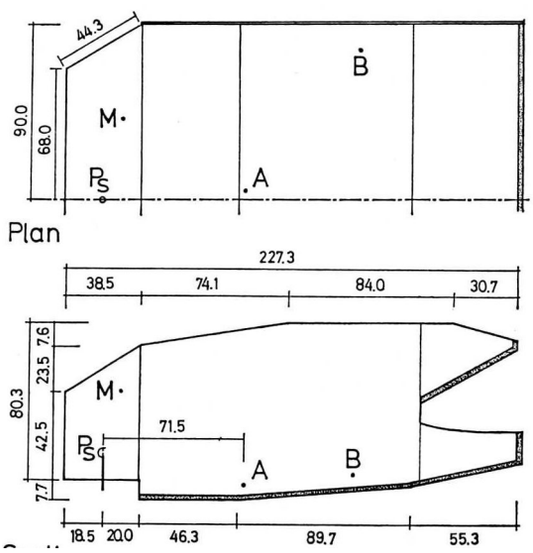

Figure 13: Scale model of an auditorium. A point source is a P_s and a reference microphone for simultaneous measuring of the direct sound is a M. Receiving points are A and B. Dimensions of the boundaries are shown in cm.

The convex ceiling is divided into three tangential rectangular plane panels in the calculation, then all the boundaries are calculated as rectangular plane panels.

Two parallel lateral walls are covered with punch-carpet layer of about 4mm thickness, the seat areas in the first floor and on the balcony, and rear walls are covered with urethane foam layer of 10mm thickness, whose reflection coefficients are shown in Figure 6. The other surfaces are made rigid. The spark pulse is generated at P_s on the stage. Wave forms were recorded on the digital memory with the sampling points 4,096 and sampling time of 10μs. For the anti- aliasing filter, low pass filter whose cut off frequency is 22.4 kHz with 24dB/oct and 28 kHz with 32dB/oct were used in series. Receiving points were at A and B in Figure 13. Receivers were two 1/4 inch condenser microphones which were recognized omni-directional below 15 kHz.

2) Comparison of measured and calculated results

Impulse responses at receiving points A and B were calculated. Discreteness of a geometrical wave was lost following the lapse of time at the calculated first reflec-tions, because edge waves become closer to it and negatively larger. It is also lost by the convolution of reflection coefficients. The second geometrical and specular reflections lost more discreteness. Because the first reflected edge waves are negative, their geometrical and most of their specular reflections are negative. They correspond to the modification of the overestimation at the second geometrical and specular reflections. The second geometrical and specular reflections of edge waves modified the overestimation at the third geometrical and specular reflections. The difference between receiving points A and B are noticed on the effect of the negative surface reflection at the ground floor. The direct sound at B is subtracted by it. In a real auditorium, such a negative surface reflection must decrease the loudness of the direct sound. The calculated impulse response up to the fourth reflections was convolved with the direct sound simultaneously measured and this is compared with the measured pulse response in Figure 14.

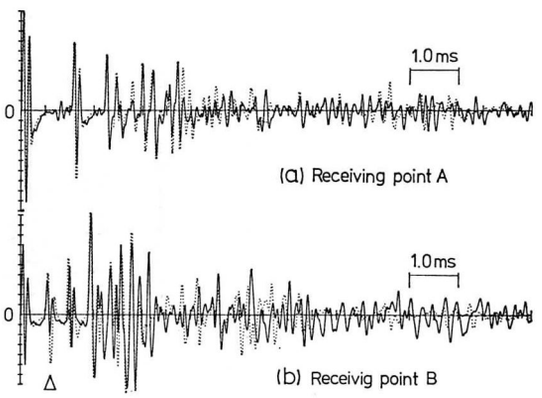

Figure 14: Pulse response of early reflections at the receiving point A and B. Solid curves are measured and dotted ones are calculated by the convolution of the first pulse wave and the calculated impulse response by sum up to the fourth reflection.

The amplitude of reflection in the ordinate is not shown, because it depends on the form and magnitude of a point source at the measurement. The disagreement, for instance, at Δ of the receiving point B in Figure 14 (b) is

caused by the excess attenuation at the edge of a panel with the thick layer of urethane foam, which cannot be predicted by Eq. (7). But it does not affect the total sound field so much. Their transfer function transformed from the pulse response until around 13ms after the direct sound is compared in Figure 15.

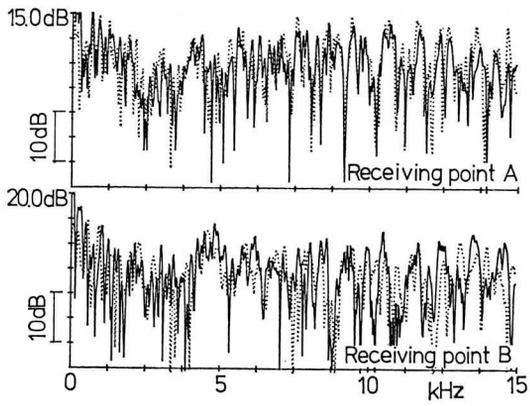

Figure 15: Measured transfer functions and the transfer functions calculated by sum up to the fourth reflection, shown by solid curve and dotted one respectively.

At a receiving point on or under the balcony, it has a few near boundaries which have specular reflection points. The decrease of the amplitude by distance from an image source is not much, in spite of the increase of the order of reflection. The early reflections such a receiving point include higher ordered reflections which are possible to be calculated by this method. These agreements show that the calculation of a sound field by geometrical acoustics is not sufficient, and that the introductions of edge waves, reflection coefficients and their multiple reflections give more precise estimation of the sound field in an auditorium.

When the sound field in an auditorium is understood as the distribution of the positive and negative image sources, the spatial information as well as the time sequence of them cannot be lost by the aid of stereo-scope expression. Then the sound field can be visualized [13].

2.4 Summary of this section

A method for calculating the early reflections of the impulse response in an auditorium is summarized based on the Terai's boundary integral equation, and on the calculation of the first reflections at boundaries and multiple reflections between them were reviewed. The result of the calculation by this method in a scale model auditorium is compared with the measured result in reasonable agreement. It is especially shown in the comparison that the multiple reflections of edge waves, which are caused by the limited dimension of the boundaries, give the effect of the modification of the overestimation caused by geometrical acoustical treatment and that reflection coefficients change incident wave forms depending on incident angles. In this way, the method on the successive substitution in the Terai's boundary integral equation shows clearly how a sound field is formed and characterized. These reflections seem to change the sound field into a diffused one and the definition of it seems to be newly discussed.

This method gives the more detailed spatial information as well as the time sequence.

3. Loudness of an impact sound

The linear part of our hearing system was found [14], having a pair comparison of the loudness of two rectangular pulses with that of a single rectangular pulse with changing their time intervals. The rectangular pulse had 0.05ms time duration, which covers our audio frequency, and had the amplitude of 93dB or 87dB.

This linear response, shown in Figure 16 is supposed to include the head related transfer function (HRTF), the elastic response of the eardrum to the three little bones, the lymph liquid in the cochlea, and the elastic movement of the basilar membrane. It might include even a part of peripheral nerve system.

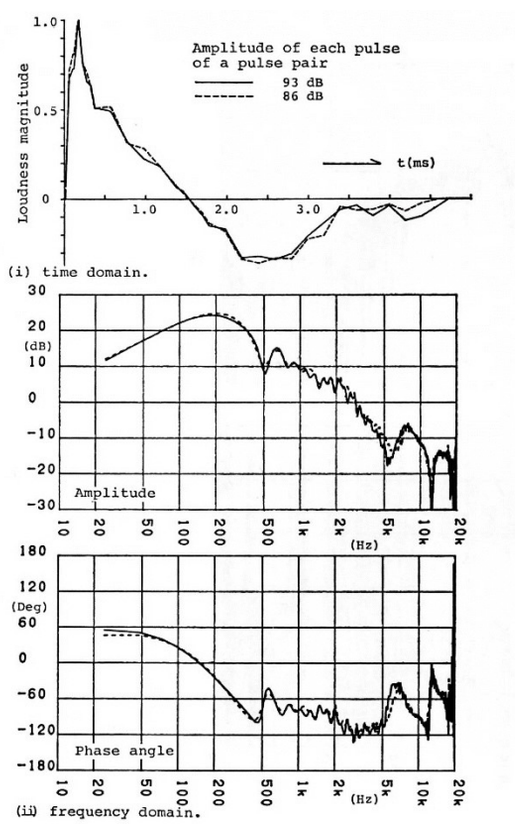

Figure 16: Impulse response of our hearing system and its frequency characteristics.

When a positive and a negative rectangular pulse of the same amplitude were given from opposite directions as in Figure 17, they were heard as the same loudness as if they were two positive rectangular pulses. It was shown that there is a process to make a sound absolutized [15] after the linear process.

It is discussed in this section how the loudness of an

impact sound is decided at the higher level. It is tried to find how it weighs on frequency and forms a time window.

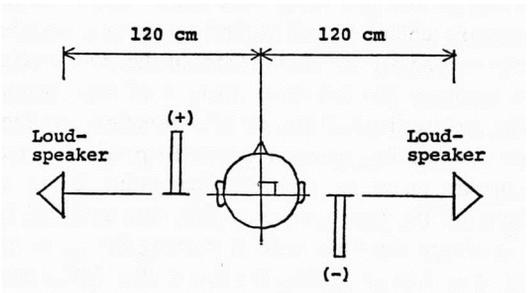

Figure 17: A positive and negative rectangular pulse from opposite directions.

1) The Thurston scale by pair comparison for various impact sounds

Firstly, eight kinds of impact noises were recorded with slight adjustment. They were the sounds of bottle tapping, concrete block hitting, tea cup tapping, aluminium bat impact, hand clapping, lighter clicking, sand-paper scrubbing and radio noise. Each impact noise got three different levels with an 8dB step and 24 impact noises were prepared. Pair comparison was done in the echoic chamber at Kansai University by 18 test persons. At pair comparison, the next pair was given at 3.5 seconds [14] after the first impact noise was ceased. The combination for a pair was not reversely done and it was the pairs of 24x23/2.

After 24 impact noises got the pair comparisons, they were arranged on the Thurston's scale in the case V and shown on one axis as in Figure18.

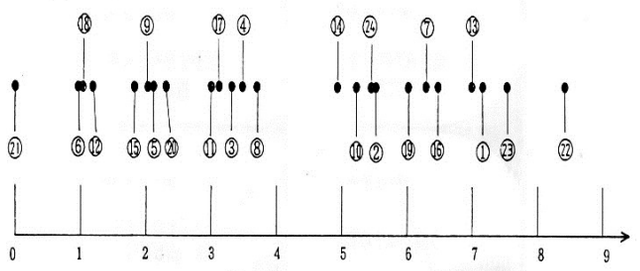

Figure 18: Loudness on the Thurston's scale for 24 impact sounds.

The next process after absolutization is supposed to have the integration in a time window. It is expressed as in the next equation (17) [16],

$$L = F\left\{\int_{t_1}^{t_2} \mid P(t) * R(t) \mid dt\right\} \qquad (17)$$

where $P(t)$ is a given sound pressure which is an impact sound here. $R(t)$ is a transient response of hearing system to be convolved. * shows convolution product. From t_1 to t_2 is the interval of a time window for the integrand. $F\{\}$ is a function of power or logarithmic. Here the latter is used practically 20log10 to get a decibel value.

2) Time window with the application of the Theory of Quantification I

Having the Thurston's scale as an outsider and a variety of time window as a factor, Theory of Quantification I was applied to see how a multiple correlation coefficient changes. It was searched which time window shows the largest multiple-correlation coefficient. It must be the most proper time window.

An impact sound is convolved with: (a) unity to have a physical impact sound, (b) "A" weight without any phase angle and (c) the impulse response of our hearing system in Figure 16. After each convolution, it is absolutized and integrated with a variety of time windows.

Time	Multiple Correlation Coef.			Time	Multiple Correlation Coef.		
window	(a)	(b)	(c)	window	(a)	(b)	(c)
10ms	0.8474	0.8399	0.9165	90ms	0.8286	0.8296	0.9181
20ms	0.8560	0.8545	0.9127	100ms	0.8211	0.8296	0.9003
30ms	0.8490	0.8500	0.9129	110ms	0.8211	0.8301	0.9003
40ms	0.8644	0.8764	0.9322	120ms	0.8216	0.8214	0.9003
50ms	0.8838	0.8855	0.9299	130ms	0.8216	0.8214	0.8957
60ms	0.8792	0.8940	0.9159	140ms	0.8216	0.8214	0.8931
70ms	0.8670	0.8291	0.9164	150ms	0.8488	0.8352	0.8931
80ms	0.8670	0.8222	0.9181	160ms	0.8488	0.8352	0.8931

Table 1: Multiple correlation coefficients by the Theory of Quantification I for three different convolution functions in the integral Eq. (17): (a) an impact sound itself; (b) "A" weight without any phase angle; and (c) the impulse response of our hearing system.

The integration with a time window was converted to the decibel value with 20log10. It was categorized with a 5dB step. Categories for convolutions (a) (b) and (c) in the above are varied 7 to 9. The result is shown in Table 1.

It shows that the largest multi-correlation coefficient among three convolving functions for every time window was with the impulse response of hearing system. Namely, it says that it is most proper weighing on our hearing attitude of an impact sound. And at the time window of 40ms the multiple-correlation coefficient is the largest for the outsider of the Thurston's scale. It must be the best time window for an impact sound.

A half of the selected impact sounds included pure tones. It was also quantified with Theory of Quantification I to have another factor for pure tone. At the time window 40ms the multiple-correlation coefficient changed only 0.9322 to 0.9357. It is not affected by the factor of pure tone. It might have been accepted as a part of the sound. There must exist a few other factors to make the coefficient larger.

3.1 Summary of this section

The loudness of an impact sound is estimated as follows:

- Firstly, the impulse response of our hearing system is convolved to a given impact noise. If it has an incident angle, its normalized directivity must be convolved.
- Before each signal comes to binaural hearing it is absolutized.
- Meantime, a path way is chosen for the signal; for instance, a pure tone from outside does not beat with a low pitch sound, the resonance frequencies at the ex-ternal ear are smoothed at the transient response for the rectangular pulse of 0.05ms. A rectangular pulse and a pure tone seem to be registered differently in brain.
- 40ms is the best time window for deciding the loudness of an impact sound.
- The non-linear function of power or logarithmic are supposed to be made with the saturation of excessive large input and the internal noise of our self, and the loudness level is given.
- A time window is supposed to be decided by the information and the auto-correlation of a given signal, and the integrand of Eq. (17) is integrated during the time window.

A sound field and the linear part of our hearing system have been solved for a rectangular pulse of 0.05ms. Accordingly, getting out somewhat confused expression of them in the frequency domain, the acoustical linear phenomena are properly arranged and grasped clearly. The above concept can be schematically expressed as in Figure.19.

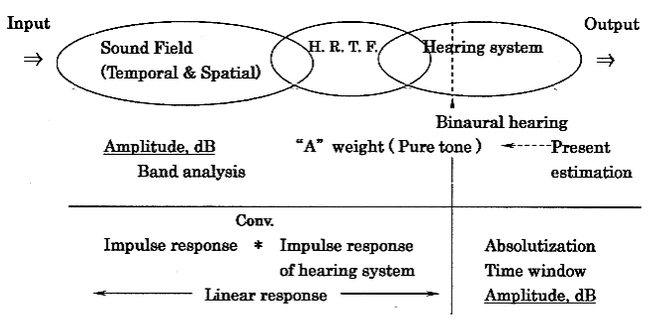

Figure 19: Sound field and hearing system

3.2 Additional comments

1) Absolutization in the hearing system and intensity

Acoustic signal travels in the linear form until it reaches to the process of absolutization of the hearing system. A diffusive sound field does not have any particular direction to hear. Energetic treatment with the amplitude of a microphone in a sound field explains a noise environment somewhat. But if a sound field is coherent or has dominant directions of incidence, it must be careful that the output of a level meter through an omni-directional microphone does not always decide the loudness. There the incident angle is important for the loudness because the HRTF is involved.

2) Temporal aspect of 0.05ms rectangular pulse

Looking back, experiments in the past with 0.05ms rectangular pulses, temporal aspect was as in the following:

0ms Two pulses of the same amplitude are heard as one pulse with interference.

...Continued on Page 16

Continued from Page 14

1.4ms	Two positive pulses of the same ampli-tude start to be heard split.
1.7ms	Two pulses in positive and negative signs of the same amplitude start to be heard split.
3.5-3.8ms	Each of two pulses of the same amplitude is heard equal. Slightly larger than that of a single pulse.
4-5ms	Two pulses are heard completely separated, but its loudness is still slightly larger.

The discrimination time of 1-3ms by Hirsh [17] is referred to papers by Wallach, Newman and Rosenzueing and it was found at different directions. On the other hand, our results in the above were obtained at the median plane.

We learnt that two rectangular pulses of 0.05ms are heard as the same loudness at the time interval of 3.5-3.8ms [14]. It means that the time window for non-correlated two pulses is finished to have integration. This must be the shortest time window. It starts to be separated at 1.4 to 1.7ms but it is not yet done by a time window. Even after this shortest time window, it is not enough long to understand the meaning of signals. They are not yet autocorrelated for that.

3) Gestalt psychology by two 0.05ms rectangular puls-es

Two successive rectangular pulses were heard three or more continuous sounds when their time interval was 50m-80ms. Two non-correlated signals make Gestalt psychology. It is interesting too because it was different at each test person. A few other persons heard them just as two pulses. This different response might tell one's musical favorite and/or talent. The inverse frequency of this range is 12-20Hz. α brain wave (EEG) has 8-13Hz, the lowest frequency of a pipe organ is 16Hz.

4) A few other things around 40ms time difference

A singer at a choir does not like the delay of 40ms from surrounding reflectors on the stage (Harold Marshall, personal communication)

The path difference with 40ms is 13.6m. For 50ms it's 17m. It is often referred this path difference to have the disturbance by an echo especially on speech.

4. Method of acoustical estimation of an Auditorium

The impulse response calculation of the early reflection in an auditorium has been established as well as its transfer function. The linear response of human hearing system was measured in the form of impulse response with a rectangular pulse of 0.05ms. When a positive and a negative pulse were given from the opposite direction, they were heard on loudness as if two positive pulses were given. It is found that they are absolutized after the linear response.

The discrimination angle for the 0.05ms rectangular pulse was measured, and it happened with the cross-correlation 0.98 of the head related transfer function (HRTF) [18]. Acoustical information can be smoothed spatially and temporally in that region, being convolved with the impulse response of our hearing system which is modified by the directivity. To find its loudness, it must be integrated in a time window.

The above information can be expressed using the stereo-scopes. It is called visual sound field [13]. One of the authors got acoustic measurements of world famous concert halls to relate such information of the early reflections of them and their reputations.

4.1 Spatial discrimination for sound field estimation

A rectangular pulse of 0.05ms was generated every one second in the anechoic chamber at Kansai University. A test person was on a rotary chair and asked when he felt that coming direction was changed. Seven centre angles were chosen from 0 degree to 180 degrees at every 30 degrees. The chair was rotated clockwise and anticlockwise. The median plane was at 0 degree and the loud speaker was rotated at 1.2 metres away from a test person.

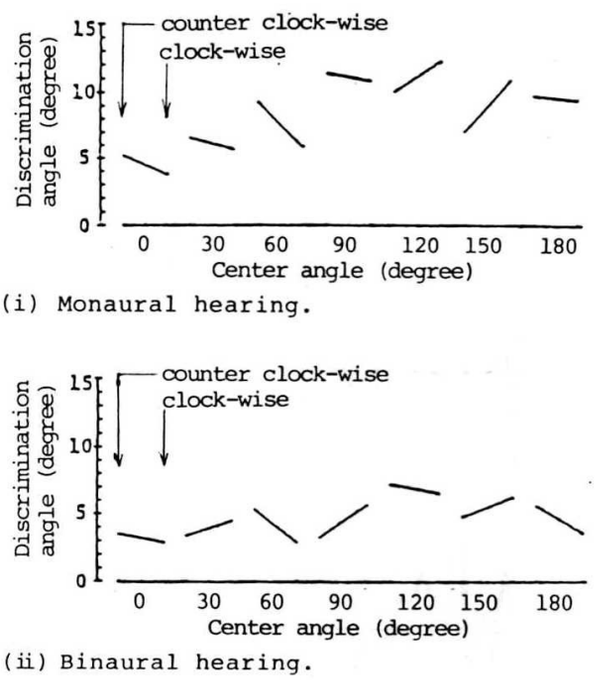

Figure 20: Threshold angle of direction discrimination to a rectangular pulse of 0.05ms at monaural and binaural hearing.

Eight male students were tested twice for each and its average was obtained. A discrimination angle is for the clockwise and anticlockwise. Threshold angle of discrimination for monaural hearing is given for each centre angle in Figure 20 (i), and that for binaural hearing in Figure 20 (ii). It is very interesting that the binaural hearing shows much more sensitive. The cross talk between both ears should be possible to explain it.

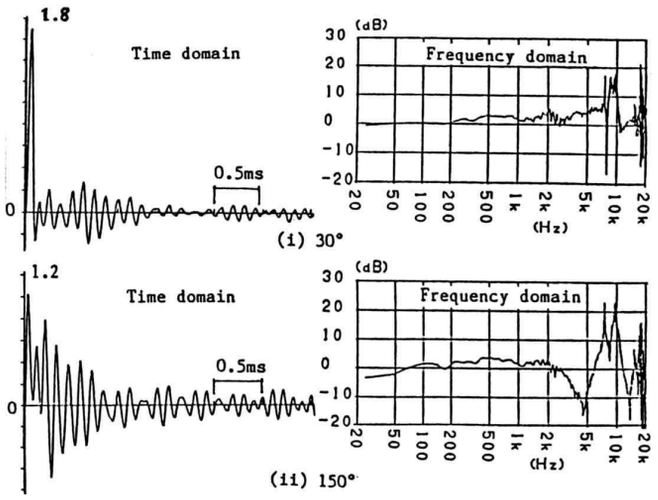

Figure 21: Directivity of head-related transfer function normalised by the one at normal incidence for the incident angle 30 degrees above and 150 degrees below.

The monaural discrimination threshold is supposed to be given by the change of head-related transfer function (HRTF). Namely, it was caused by the cross-correlation function between the HRTF at the centre angle and the discriminated angle. HRTF was measured at the eardrum of a dummy head at a different incident angle with the rectangular pulse of 0.05ms.

The directivity of the HRTF at 30 degrees and 150 degrees is shown in Figure 21 as examples after it was de-convolved or normalized with the one at the front incidence. They are shown for the time domain in the left and the frequency domain in the right.

The transient response of our hearing system, usually written by $R(t)$, was measured at the front. If $R(t)$ is convolved with the directivity at an incident angle, the transient response of our hearing system of the angle is obtained. When directivity is expressed in the time domain being de-convolved with the front one, it can be clearer to understand its feature and it is the information enough for the direction.

As the angle discrimination was supposed to be caused by the directivity of HRTF, the maximum value of the cross

correlation function between the directivity at a centre angle and the one at the angle when it was felt changed, was discussed. It was normalized by the auto-correlation function of the two functions.

The maximum cross correlation for each centre angle is shown in Figure 22 for clockwise with 'o' and counter clockwise with 'x'. It deviates around 0.98. The result in Figure 22 was obtained from the experiment in the horizontal level. It is evident that the discrimination is strongly depending on the directivity of the HRTF. If the directivity of a dummy head for a different angle is obtained and the space is divided with angles where cross correlation is 0.98, the spatial discrimination angle will be found for the whole space.

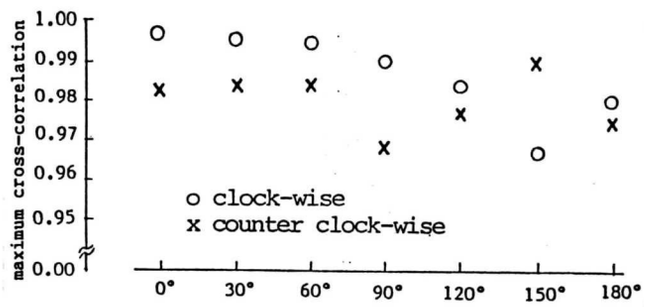

Figure 22: Relation between the threshold of angle discrimination with the maximum cross-correlation of the head-related transfer function.

The sound field information on the impulse response is separated in the angle and then the transient response of hearing system modified to the angle is convolved to it. The acoustic information is smoothed and easier to discuss with.

Not only in the time domain for the evaluation of an auditorium, must it be discussed with the spatial information together. A visual sound field was introduced with stereoscopic expression [13].

4.2 Summary of this section

- Calculation of the impulse response of an auditorium to see it spatially in the time domain.
- Convolution to it of the impulse response of hearing system with the directivity-modified HRTF in a discrimination angle: The space must have 0.98 on the cross correlation of HRTF.
- Integration of its absolute value in the time window 40ms for loudness as a temporary time window.
- The loudness in each discrimination angle is calculated in every time window. This loudness of reflections is expressed in the time sequence through the auditorium space.
- Using visual sound field to see the reflections in loudness, its change can be observed from one seat to another. Reputation of each seat is referred to the visual sound field to find the common Acoustical characters.

When one of the authors got sabbatical leave in 1985 to 1986, he visited world famous concert halls for acoustical measurements. They were done with impulsive sound sources on the stage to a several audience seats. Their impulse responses will be obtained with their Architectural drawings.

Acknowledgements

The authors appreciate Ms Fumiko Nantani for her help of copying some materials from our past papers to MSWord.

References

1. T. Terai, "On calculation of sound fields around three dimensional objects by integral equation meth-ods," J. Sound Vib. 69, 71-100(1980).
2. E. J Skudrzyk, The Foundation of Acoustics (Springer-Verlag, Wien, New York, 1971), p. 517-524.
3. K. Miyamoto, "New representation of wave field," Proc. Phys. Soc. 79, 617-629 (1962).
4. Y. Sakurai and K. Nagata, "Sound reflections of a rigid plane panel and of the 'live end' composed by those panels," J. Acoust. Soc. Jpn. (E) 2, 5-14 (1981).
5. Y. Sakurai, "Sound reflection of a curved rigid pan-el," J. Acoust. Soc. Jpn. (E) 2, 63-70 (1981).
6. Y. Sakurai, and K. Nagata, "Practical estimation of sound reflection of a panel with reflection coefficient," J. Acoust. Soc. Jpn. (E) 3, 7-15 (1982).
7. Y. Sakurai, H. Morimoto and K. Ishida; "The re-flection of sound at grazing angle by auditorium seats", Applied Acoustics, 39, 209-227 (1993).
8. L. W. Cremer, Auditorium Acoustics, ed. by R. Mackenzie (Applied Science, London, 1975), pp. 145-150.
9. Y. Sakurai and K. Ishida, "Multiple reflections be-tween rigid plane panels," J. Acoust. Soc. Jpn. (E) 3, 183-190 (1982).
10. Y. Sakurai and K. Ishida, "Multiple reflections between rigid curved panels, "J. Acoust. Soc. Jpn. (E) 4, 27-33 (1982).
11. Y. Sakurai and K. Ishida, "Multiple sound reflec-tions between plane panels covered with reflection coefficients," J. Acoust. Soc. Jan. (E) 4, 121-126 (1983).
12. Y. Sakurai: "The early reflection of the impulse response in an auditorium", p127-138, J. Acoust. Soc. Jpn. (E), 8, 4 (1987).
13. Y. Sakurai, "Visual sound field," 11th I.C.A. (Paris), Vol. 4, 437-440 (1983).
14. Y. Sakurai and H. Morimoto:" The transient re-sponse of human hearing system", J. Acoust. Soc. Jpn. (E), 10, 4, p221-228 (1989).
15. Y. Sakurai and H. Morimoto: "Binaural hearing and time window in the transient", J. Acoust. Soc. Jpn.(E), 10, 4, p229-233, 1989.
16. H. Morimoto and Y. Sakurai: "Loudness of an impact sound", J. Temporal Design in Architecture and the environment, vol.12, No1, p83-91, 2014.
17. I. J. Hirsh: "Temporal aspects of hearing", in The Nervous System, Vol. III Human Communication and its Disorders, E. L. Eagles, Ed. (Raven Press, New York, 1075), p157-162.
18. H. Morimoto and Y. Sakurai: "Method of acous-tical estimation of an auditorium", J. Temporal Design in Architecture and the environment, vol.12, No1, p83-91, 2014.